Nuclear Instruments and Methods in Physics Research A ∎ (∎∎∎∎) ∎∎∎–∎∎∎

Contents lists available at SciVerse ScienceDirect

Nuclear Instruments and Methods in Physics Research A

journal homepage: www.elsevier.com/locate/nima

Ferroelectric plasma sources for NDCX-II and heavy ion drivers

E.P. Gilson [a,*], R.C. Davidson [a], P.C. Efthimion [a], I.D. Kaganovich [a], J.W. Kwan [b], S.M. Lidia [b], P.A. Ni [b], P.K. Roy [b], P.A. Seidl [b], W.L. Waldron [b], J.J. Barnard [c], A. Friedman [c]

[a] Princeton Plasma Physics Laboratory, Princeton University, P.O. Box 451, Princeton, New Jersey, 08543, USA
[b] Lawrence Berkeley National Laboratory, One Cyclotron Road, Berkeley, California, 94720, USA
[c] Lawrence Livermore National Laboratory, P.O. Box 808, Livermore, California, 94550, USA

ARTICLE INFO

Keywords:
Plasma sources
Neutralized transport
Beam neutralization

ABSTRACT

A barium titanate ferroelectric cylindrical plasma source has been developed, tested and delivered for the Neutralized Drift Compression Experiment NDCX-II at Lawrence Berkeley National Laboratory (LBNL). The plasma source design is based on the successful design of the NDCX-I plasma source. A 7 kV pulse applied across the 3.8 mm-thick ceramic cylinder wall produces a large polarization surface charge density that leads to breakdown and plasma formation. The plasma that fills the NDCX-II drift section upstream of the final-focusing solenoid has a plasma number density exceeding 10^{10} cm^{-3} and an electron temperature of several eV. The operating principle of the ferroelectric plasma source are reviewed and a detailed description of the installation plans is presented. The criteria for plasma sources with larger number density will be given, and concepts will be presented for plasma sources for driver applications. Plasma sources for drivers will need to be highly reliable, and operate at several Hz for millions of shots.

1. Introduction

In order to compress space–charge-dominated ion beams and deliver high fluence beams to high energy density laboratory plasma (HEDLP) targets and heavy ion fusion (HIF) targets, the beam space–charge must be neutralized. In ion-beam-driven HEDLP and HIF scenarios, an accelerator generates a high density, high energy beam, and arranges the beam's phase space such that, in the absence of space–charge and thermal effects, the beam would drift ballistically to a focus at which all particles would arrive simultaneously. Thermal emittance effects can be minimized by careful and deliberate manipulation of the beam in the accelerator. The repulsive effects of space–charge can be mitigated by allowing the ion beam to pass through a large-volume plasma that acts as a reservoir of neutralizing electrons, in the case of a positively charged ion beam. These plasma sources must not otherwise interfere with beam propagation.

Theory, modeling, simulation, and experiments in this area have been carried out under the auspices of the Heavy Ion Fusion Science Virtual National Laboratory (HIFS-VNL). Experiments have been carried out at Lawrence Berkeley National Laboratory (LBNL) on the Neutralized Transport Experiment (NTX) and the Neutralized Drift Compression Experiment–I (NDCX-I). These experiments demonstrated the feasibility of using a large-volume, dense plasma to neutralize the space–charge of a 300 keV singly ionized potassium ion beam and allow it to focus longitudinally and transversely to a small spot size. While the NDCX-I facility was able to carry out experiments using beams with high perveances that are relevant to heavy ion fusion driver systems, the facility was not designed to create target density and temperatures corresponding to a warm dense matter (WDM) state, nor did it allow detailed studies of beam target interactions near the Bragg peak of the energy deposition curve.

The NDCX-II facility is a new user facility operated by the HIFS-VNL at LBNL that will create target conditions corresponding to the WDM regime, and also lead to the development of an improved fundamental understanding of the physics that governs the process of neutralized drift compression and beam–plasma interactions with application to heavy ion fusion [1–4]. Plasma sources have been designed and built for NDCX-II to ensure that sufficient plasma will be available for beam charge-neutralization. In this paper, the NDCX-II plasma sources used upstream of the final focus solenoid are discussed, as well as progress on optimizing and improving them. The plasma source requirements for a full-scale HIF driver system are also discussed.

2. NDCX-II plasma requirements

The NDCX-II ion beam is a singly ionized lithium beam in which 50 nC charge bunches will have a radius of approximately 2 cm and a length under 20 cm when they exit the final cell of the acceleration and transport section with an average kinetic energy

* Corresponding author.
E-mail address: egilson@pppl.gov (E.P. Gilson).

0168-9002/$ - see front matter © 2013 Elsevier B.V. All rights reserved.
http://dx.doi.org/10.1016/j.nima.2013.05.091

of 1.2 MeV. These parameters correspond to a beam number density in the 10^9 cm^{-3} range and an effective pulse duration of approximately 30 ns. However, at this point in the machine, the beam will have been given a strong velocity tilt so that the head of the beam is traveling more slowly, while the tail of the beam is traveling more quickly. Thus, as the beam drifts through the meter-long neutralized drift region of NDCX-II, the beam bunch will be compressing longitudinally, with the number density increasing linearly along the drift length. When the beam reaches the entrance of the 8 T final focusing solenoid, it will have compressed longitudinally to a length of under 4 cm, thereby increasing the peak beam density to the 10^{10} cm^{-3} range.

While the beam will continue to compress longitudinally, the 8 T final focus solenoid will cause the beam bunch to begin compressing radially. Therefore, the beam ion number density will increase rapidly after the beam bunch emerges from the final focus magnet and drifts towards the target plane. The result of the simultaneous longitudinal and radial compression of the beam is a beam bunch at the target plane that has a radius that is less than 0.5 mm and a length that is nearly 0.5 cm, corresponding to a pulse duration of 1 ns. At the target plane, the beam density is expected to be in the 10^{13} cm^{-3} range, perhaps approaching 10^{14} cm^{-3}. Fig. 1 shows the approximate expected peak beam density along a one-meter-long neutralized drift region in NDCX-II. Here, the final focus solenoid is taken to be a thin lens placed 0.8 m along the drift length. Note that while the curve in this figure is illustrative and based on a simple geometric model of a compressing beam, it is nonetheless consistent with ASP and WARP simulations of the expected NDCX-II beam performance [5].

The beam density is not expected to exceed 10^{11} cm^{-3} upstream of the final focusing solenoid; therefore, in this region, the ferroelectric plasma source used on NDCX-I serves as the basis for the NDCX-II plasma source because it routinely generates plasmas with number densities in the mid-10^{10} cm^{-3} range. In the NDCX-II target chamber, where the beam density will be greater, the quartet of cathodic arc plasma sources that was used on NDCX-I will be used to provide plasma within the final focus solenoid, downstream of the solenoid, and near the target plane on NDCX-II [3,6].

3. Ferroelectric plasma source

A plasma source based on high-dielectric ceramics was selected for the drift region upstream of the final focus solenoid because such a source can generate sufficiently dense plasma without the introduction of extraneous electric or magnetic fields, and without the addition of any feedstock gas into the system [7,8]. Barium titanate is a ceramic with a relative dielectric coefficient of several thousand. When a voltage is applied across a slab of this material using a pulser configuration such as the one shown in the simplified schematic in Fig. 2, a large polarization surface charge density is created. If the electrodes that are used to apply the voltage are not solid, but instead leave a region of the ceramic surface exposed, then tangential electric fields are formed at the ceramic/electrode/vacuum interface. For example, these electrodes could be formed using perforated metal sheet, or strips of metallic tape with conductive adhesive.

These strong electric fields lead to an initial breakdown of the surface material and the electrode material. The plasma propagates along the ceramic surface with the uncompensated bound polarization surface charge density effectively neutralized by the plasma. Particle fluxes from the propagating plasma to the ceramic surface lead to the emission of adsorbed gas, ceramic material, and electrons from the surface. Ionization of the adsorbed gas and ceramic material leads to the formation of a secondary plasma. The mechanisms involved in the formation of the plasma and the composition and plasma properties of the resulting plasma are still under both experimental and theoretical investigation [9].

Plasma sources based on the NDCX-I ferroelectric plasma source design [10,11] have been built and delivered to the NDCX-II facility for installation (see Fig. 3). The NDCX-II sources are made using barium titanate cylinders that have an 8.38 cm outer diameter, a 7.62 cm inner diameter, and are 4.06 cm long. These cylinders have a silver coating on their outer surface that serves as the high-voltage electrode. Perforated steel strips approximately 2.5 cm in width are rolled and inserted into each cylinder to form the inner electrode where plasma formation occurs. Up to five cylinders can be stacked together, wrapped in a copper jacket, and held together by thin wires strung back and forth axially along the inner surface between two aluminum end rings to form a plasma source module. Insulating white delrin end collars prevent high-voltage arcing at the ends of the module. Protective kapton strips have been added to the interior surface of the plasma source modules at the interfaces between adjacent ceramic cylinders to eliminate high-voltage failures between cylinders. Thyratron-switched pulsers with 150 nF of storage capacitance charged to 7 kV are used to drive the plasma source

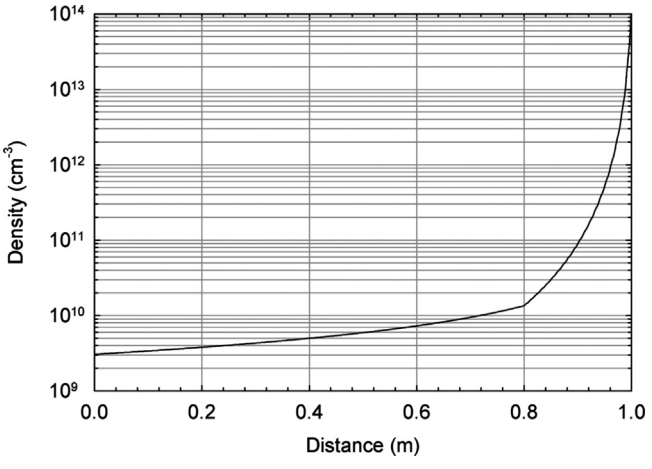

Fig. 1. The ion beam density plotted as a function of drift distance for a simple model in which the bunch length decreases linearly with distance and the radius is constant until 0.8 m, after which the radius decreases linearly with propagation distance. Here, a 50 nC charge bunch is assumed with a 2 cm initial radius and a 0.5 mm final radius.

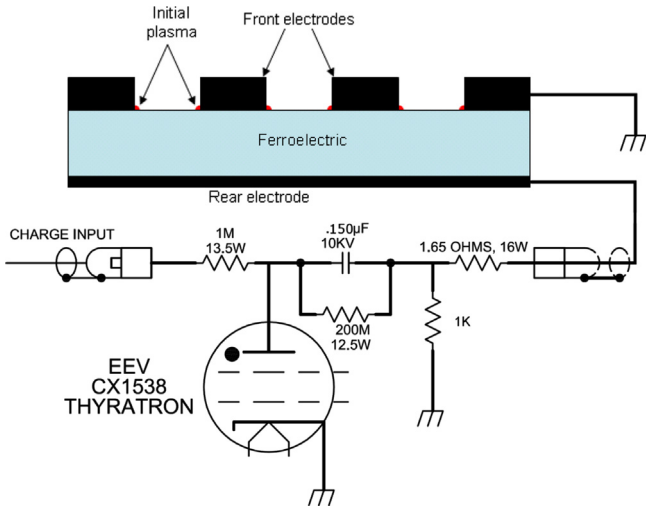

Fig. 2. A schematic drawing of the ferroelectric plasma source and its thyratron-switched pulser. The 150 nF storage capacitor is charged to high positive voltage, and when the thyratron switch is triggered, a large negative voltage appears on the rear electrode of the ferroelectric material.

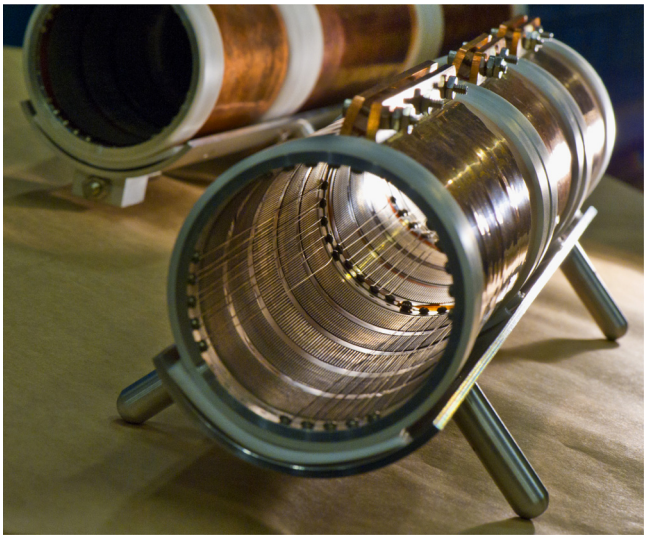

Fig. 3. The NDCX-II ferroelectric plasma source. The plasma source is assembled using 4.06 cm-long barium titanate rings that are stacked together to form modules of various lengths. Each ring is fitted with a rolled strip of perforated steel sheet that forms the inner electrode. Thin wires are drawn axially along the inner surface to ground the inner electrodes and to hold the module together. The high-voltage pulse is applied to the copper jacket that surrounds the exterior of the module.

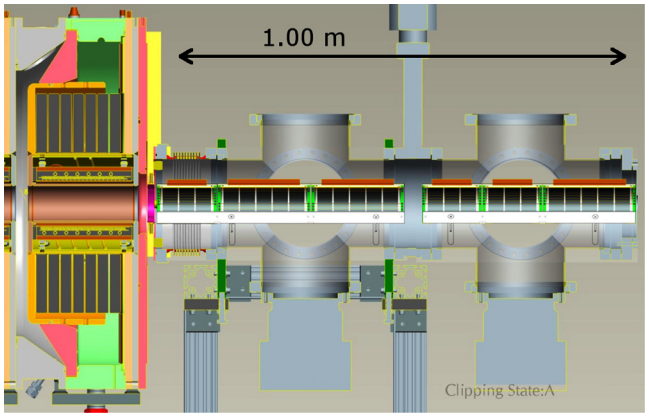

Fig. 4. A schematic of the proposed drift section of NDCX-II, in which the beam propagates from left to right, shows the final cell on the left with its stack of ferrite cores that drives the induction gap, and its pulsed solenoid for beam transport. The ferroelectric plasma source modules sit on aluminum cradles inside a bellows, two crosses, and a gate valve. To integrate properly with the system hardware, the plasma source modules shown here are constructed with three, five, five, three, three, and five rings.

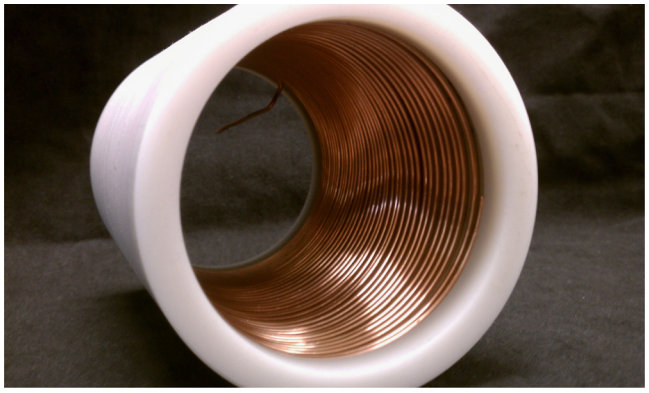

Fig. 5. A prototype ferroelectric plasma source with a white delrin outer jacket that holds the module assembly together axially and insulates the high voltage applied to the outer surface from the chamber wall. The inner electrode is made from a continuous helical copper winding to create better contact with the ceramic wall and provide increased electrode spacing.

modules. In this way, plasmas are created with number densities in the mid-10^{10} cm^{-3} range that persist for tens of microseconds.

The number of modules and the lengths of the individual modules were determined during the NDCX-II design process in order to integrate simply with the system. For example, a gate valve must be included in the NDCX-II system at a location downstream of the final cell so that target chamber can be opened for target insertion and maintenance without venting the entire accelerator. Effective neutralization of the ion beam by the plasma electrons is critical, and so the gate valve is not placed between the final cell and the ferroelectric plasma source, but rather at a location that is approximately half way along the neutralized drift region. Fig. 4 shows the layout of the planned installation of the ferroelectric plasma source on NDCX-II. The plasma source entrance is placed immediately downstream of the final cell, and the lengths of the modules are designed to fit within standard vacuum bellows and crosses. Aluminum cradles (see Fig. 3) support the plasma sources and center them with respect to the beam axis. Not shown in Fig. 4 are the final focusing solenoid and target chamber that sit downstream of the ferroelectric plasma source.

While these plasma sources will provide sufficient plasma for NDCX-II experiments, improvements to the ferroelectric plasma source design are being explored in order to increase the maximum achievable plasma density, and increase the lifetime of the plasma source nevertheless. Fig. 5 is a photograph of a modified three-ring ferroelectric plasma source. To improve the high-voltage standoff capability, the delrin end collars have been redesigned to completely encase the outside surface of the plasma source. Only a small tab (not visible in Fig. 5) protrudes for applying the high-voltage pulse. Further, the exterior delrin enclosure is made as two threaded pieces that connect in order to provide the axial compression required to hold together the stack of ceramic cylinders. The rolled perforated steel sheets that lined the inner surface of each ceramic ring have been replaced with a single, continuous helical copper winding. Acting as a torsion spring, the copper coil uniformly presses against the walls of the ceramic rings. Either end of the copper coil can serve as the ground connector. The kapton strips that cover the interfaces between adjacent ceramic rings are especially important since the copper coil passes directly over the interfaces between ceramic cylinders. The pitch of the copper winding is chosen so that the spacing between turns is approximately 2 mm. This is significantly larger than the hole size of the perforated steel sheet and allows for the plasma to expand along the surface of the cylinder.

The combination of improved electrode contact with the ceramic wall and larger electrode spacing both lead to improved plasma source performance. In Fig. 6, black marks indicating localized plasma formation sites can be seen in photographs of sections of the barium titanate ceramic ring interior walls for the cases when the perforated steel sheet insert was used [Fig. 6 (left)] and when the helical copper winding was used [Fig. 6 (right)]. When the perforated steel sheet was used, the regular square grid of the perforations is visible, but the marks are faint and nonuniform. In contrast, when the helical copper winding is used, the black marks are darker, and also reasonably uniform along the length of the copper coil. This suggests that more point-like plasma discharges are formed using the modified plasma source design, leading to a larger total plasma density. These black marks can be cleaned from the ceramic ring surface and the electrode with sandpaper and, because there is no visible damage to either the ceramic or the electrode after cleaning, it is not clear whether the black marks represent ceramic erosion or electrode erosion. The performance and lifetime of the plasma source are not

Please cite this article as: E.P. Gilson, et al., Nuclear Instruments & Methods in Physics Research A (2013), http://dx.doi.org/10.1016/j.nima.2013.05.091

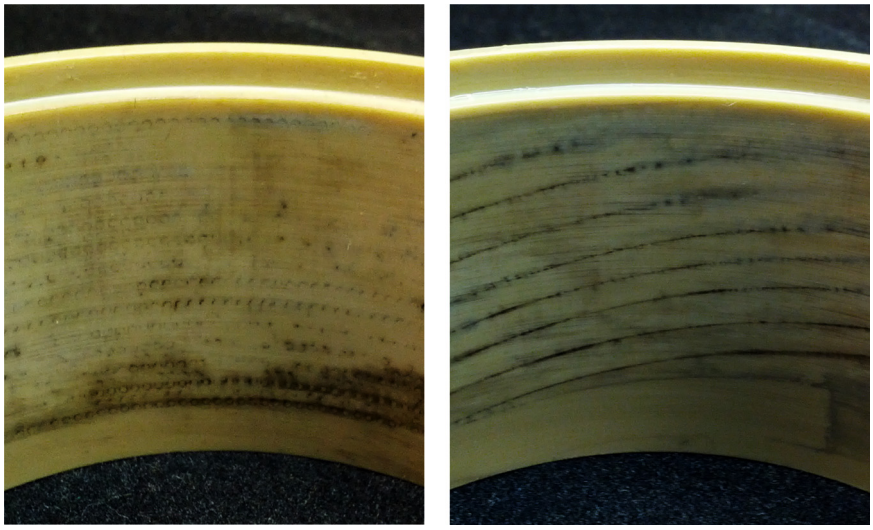

Fig. 6. (left) A faint regular square grid pattern is visible on the interior of a barium titanate ceramic ring after the perforated steel sheet electrode is removed. The black marks indicate the locations of plasma formation. (right) A clear series of black marks visible after the copper coil is removed show that the copper coil provides better contact, allowing for more uniform and dense plasma emission.

presently limited by the formation of these black marks, but rather by occasional bulk failure of the ceramic material or high-voltage breakdown due to degraded insulation.

4. Heavy ion fusion driver requirements

Heavy ion fusion drivers will generate beams of considerably greater energy than NDCX-II and, thus, be substantially larger facilities. For example, heavy ion fusion drivers, such as those described in the Robust Point Design [12], will include kilometers-long accelerators followed by drift compression sections that will be hundreds of meters long. This driver design concept makes use of multiple ion sources and injectors to create over 100 beams of 1.6 MeV singly ionized bismuth ions that are accelerated to 4 GeV, after which the beams undergo drift compression before entering the target chamber. During this drift compression, the beams increase in peak current from under 100 A per beam to approximately 2 kA per beam. If, for example, initial and final beam radii of 4 cm and 1 mm are assumed, the corresponding peak beam densities at the beginning and end of the drift compression region are 10^{10} cm^{-3} and 10^{14} cm^{-3} respectively.

While the NDCX-II ferroelectric plasma sources already create plasmas with densities of 10^{10} cm^{-3}, it is also possible that they will be able to generate plasmas with densities approaching 10^{14} cm^{-3} in order to meet driver requirements. Modification of the plasma source pulser waveform shape is being studied as a method for increasing the plasma density by rapidly changing the applied voltage using crowbar circuits. Improved plasma source module engineering and ceramic material manufacturing methods may allow for higher charging voltages to be used, leading to higher plasma density without high-voltage breakdown. The modular nature of the ferroelectric plasma source implies that it can be scaled from the one-meter drift length of NDCX-II to the drift length of a driver system. Moreover, plasma sources in a driver would be required to have repetition rates of several Hz, and this is achievable by increasing the performance of the plasma source charging and energy storage systems. The plasma source repetition rate is not limited by the properties of the barium titanate ceramic material.

However, if, for practical energy production purposes, reactor outages are limited to one per year, then plasma sources operating at several Hz must be able to function for 10^8 shots. Present ferroelectric plasma sources typically operate for 10^5 shots before refurbishment or repair is needed. Therefore, studies will be carried out to determine whether or not improved plasma source design, engineering, and material quality control can contribute to extended plasma source lifetimes. With continued development and improvement, ferroelectric plasma sources may be well-suited for heavy ion fusion driver applications.

5. Conclusion

Ferroelectric plasma sources developed for NDCX-I are well-suited for use on NDCX-II. They are capable of providing plasmas with densities in the 10^{10} cm^{-3} range for 10 μs durations in order to create a large-volume source of neutralizing electrons for the NDCX-II lithium ion beam as it travels from the exit of the final cell to the entrance of the 8 T final focusing solenoid. To improve the plasma source performance, the outer jacket has been redesigned and the inner electrode design has been optimized to enable higher density plasma generation. The current-generation ferroelectric plasma sources may also be adequate for certain heavy ion fusion driver schemes, but improvements must be made to increase the plasma density and lifetime of the plasma source. Finally, while ferroelectric plasma sources may be useful in the neutralized drift section of a heavy ion fusion driver, it must be acknowledged that beam neutralization in the environment of a heavy ion fusion reactor chamber remains a difficult problem.

Acknowledgements

The authors thank Prof. Ya. E. Krasik for valuable support and technical discussions. This work is supported by the U.S. Department of Energy.

References

[1] A. Friedman, J.J. Barnard, R.H. Cohen, D.P. Grote, S.M. Lund, W.M. Sharp, A. Faltens, E. Henestroza, J.Y. Jung, J.W. Kwan, E.P. Lee, M.A. Leitner, B.G. Logan, J.-L. Vay, W.L. Waldron, R.C. Davidson, M. Dorf, E.P. Gilson, I.D. Kaganovich, Physics of Plasmas 17 (2010) 056704.
[2] A. Friedman, J. Barnard, R. Briggs, R. Davidson, M. Dorf, D. Grote, E. Henestroza, E. Lee, M. Leitner, B. Logan, A. Sefkow, W. Sharp, W. Waldron, D. Welch, S. Yu, Nuclear Instruments and Methods in Physics Research Section A 606 (2009) 6.
[3] P.K. Roy, P.A. Seidl, A. Anders, F.M. Bieniosek, J.E. Coleman, E.P. Gilson, W. Greenway, D.P. Grote, J.Y. Jung, M. Leitner, S.M. Lidia, B.G. Logan, A.

Please cite this article as: E.P. Gilson, et al., Nuclear Instruments & Methods in Physics Research A (2013), http://dx.doi.org/10.1016/j.nima.2013.05.091

B. Sefkow, W.L. Waldron, D.R. Welch, Nuclear Instruments and Methods in Physics Research Section A 606 (2009) 22.
[4] P. Seidl, A. Anders, F. Bieniosek, J. Barnard, J. Calanog, A. Chen, R. Cohen, J. Coleman, M. Dorf, E. Gilson, D. Grote, J. Jung, M. Leitner, S. Lidia, B. Logan, P. Ni, P. Roy, K.V. den Bogert, W. Waldron, D. Welch, Nuclear Instruments and Methods in Physics Research Section A 606 (2009) 75.
[5] W.M. Sharp, A. Friedman, D.P. Grote, E. Henestroza, M.A. Leitner, W.L. Waldron, Nuclear Instruments and Methods in Physics Research Section A 606 (2009) 97.
[6] A. Anders, M. Kauffeldt, P. Roy, E. Oks, IEEE Transactions on Plasma Science 39 (2011) 1386.
[7] A. Dunaevsky, Y.E. Krasik, J. Felsteiner, A. Sternlieb, Journal of Applied Physics 90 (2001) 3689.
[8] G. Rosenman, D. Shur, Y.E. Krasik, A. Dunaevsky, Journal of Applied Physics 88 (2000) 6109.
[9] V.T. Gurovich, Y.E. Krasik, V. Raichlin, J. Felsteiner, I. Haber, Journal of Applied Physics 106 (2009) 053301.
[10] P.C. Efthimion, E.P. Gilson, L. Grisham, R.C. Davidson, B.G. Logan, P.A. Seidl, W. Waldron, Nuclear Instruments and Methods in Physics Research Section A 606 (2009) 124.
[11] E.P. Gilson, R.C. Davidson, P.C. Efthimion, J.Z. Gleizer, I.D. Kaganovich, Y.E. Krasik, Laser and Particle Beams 30 (2012) 435.
[12] S.S. Yu, W.R. Meier, R.P. Abbott, J.J. Barnard, T. Brown, D.A. Callahan, C. Debonnel, P. Heitzenroeder, J.F. Latkowski, B.G. Logan, S.J. Pemberton, P.F. Peterson, D.V. Rose, G.-L. Sabbi, W.M. Sharp, D.R. Welch, Fusion Science and Technology 44 (2003) 266.

Please cite this article as: E.P. Gilson, et al., Nuclear Instruments & Methods in Physics Research A (2013), http://dx.doi.org/10.1016/j.nima.2013.05.091